

CD58 loss in tumor cells confers functional impairment of CAR T cells

Tracking no: ADV-2022-007891R2

Xin Yan (Nankai University, China) Deyun Chen (Chinese PLA General Hospital, China) Xinran Ma (Chinese PLA General Hospital, China) Yao Wang (Institute of Basic Medicine, School of Life Sciences, Chinese PLA General Hospital, China) Yelei Guo (Chinese PLA General Hospital, China) Jianshu Wei (Chinese PLA General Hospital, China) Chuan Tong (Chinese PLA General Hospital, China) Qi Zhu (Chinese PLA General Hospital, China) Yuting Lu (Chinese PLA General Hospital, China) Yang Yu (Chinese PLA General Hospital, China) Zhiqiang Wu (Chinese PLA General Hospital, China) Weidong Han (Chinese PLA General Hospital, China)

Abstract:

Chimeric antigen receptor (CAR) T-cell therapy has achieved significant success in treating a variety of hematologic malignancies, but resistance to this treatment in some patients limited its wider application. Using an unbiased genome-wide CRISPR/Cas9 screening, we identified and validated loss of CD58 conferred immune evasion from CAR T cells in vitro and in vivo. CD58 is a ligand of the T cell costimulatory molecule CD28, and CD58 mutation or downregulated expression is common in hematological tumors. We found that disruption of CD58 in tumor cells induced the formation of suboptimal immunological synapse (IS) with CAR T cells, which conferred functional impairment of CAR T cells, including the attenuation of cell expansion, degranulation, cytokine secretion and cytotoxicity. In summary, we describe a potential mechanism of tumor intrinsic resistance to CAR T-cell therapy and suggest that this mechanism may be leveraged for developing therapeutic strategies to overcome resistance to CAR T-cell therapy in B-cell malignancies.

Conflict of interest: No COI declared

COI notes:

Preprint server: No;

Author contributions and disclosures: X.Y., D.C., Y.W., Z.W. and W.H. designed the study. X.Y., D.C., X.M. and Y.W. performed the experiments. Y.W., Y.G., J.W., Q.Z., Y.L., Y.Y. and C.T. assisted with the experiments. X.Y. and D.C., Z.W., and W.H. analysed the data and wrote the original manuscript. All authors reviewed the manuscript.

Non-author contributions and disclosures: No;

Agreement to Share Publication-Related Data and Data Sharing Statement: All data that support the findings of this study are available to the researchers on reasonable request

Clinical trial registration information (if any):

CD58 loss in tumor cells confers functional impairment of CAR T cells

Xin Yan^{1, 2†}, Deyun Chen^{1†}, Xinran Ma^{1, 2†}, Yao Wang^{1†}, Yelei Guo¹, Jianshu Wei¹, Chuan Tong¹, Qi Zhu¹, Yuting Lu¹, Yang Yu⁴, Zhiqiang Wu^{1*}, Weidong Han^{1, 2, 3*}

¹Department of Bio-therapeutic, the First Medical Center, Chinese PLA General Hospital, Beijing, China

²School of Medicine, Nankai University, Tianjin, China

³National Clinical Research Center for Hematologic Diseases, the First Affiliated Hospital of Soochow University

⁴Department of Transfusion Medicine, the First Medical Center of Chinese PLA General Hospital, Beijing, China

[†]These authors contributed equally: Xin Yan, Deyun Chen, and Xinran Ma and Yao Wang

*Correspondence to: Zhiqiang Wu (wuzhiqiang1006@163.com) and Weidong Han (hanwdrsw@163.com)

Data availability

All data that support the findings of this study are available to the researchers on reasonable request. The RNA sequencing data reported in this article have been deposited in the Gene Expression Omnibus database (accession number GSE201970).

Abstract

Chimeric antigen receptor (CAR) T-cell therapy has achieved significant success in treating a variety of hematologic malignancies, but resistance to this treatment in some patients limited its wider application. Using an unbiased genome-wide CRISPR/Cas9 screening, we identified and validated loss of CD58 conferred immune evasion from CAR T cells in vitro and in vivo. CD58 is a ligand of the T cell costimulatory molecule CD28, and CD58 mutation or downregulated expression is common in hematological tumors. We found that disruption of CD58 in tumor cells induced the formation of suboptimal immunological synapse (IS) with CAR T cells, which conferred functional impairment of CAR T cells, including the attenuation of cell expansion, degranulation, cytokine secretion and cytotoxicity. In summary, we describe a potential mechanism of tumor intrinsic resistance to CAR T-cell therapy and suggest that this mechanism may be leveraged for developing therapeutic strategies to overcome resistance to CAR T-cell therapy in B-cell malignancies.

Key points:

1. We emphasized the potential critical role of CD58 loss in resistance to CAR T-cell therapy.
2. Loss of CD58 caused inefficient IS formation with CAR T cells, impairing the activation and cytotoxic function of CAR T cells.

49

50 **Introduction**

51 Chimeric antigen receptor (CAR) T-cell therapy has demonstrated
52 unprecedented success in the treatment of B-cell malignancies, especially
53 CD19-targeted CAR T-cell therapy for acute lymphoblastic leukemia (ALL) and
54 diffuse large B-cell lymphoma (DLBCL).¹⁻⁵ Notwithstanding some progress
55 achieved, primary or acquired resistance to the treatment still occurs.^{1,6} A
56 deeper exploration for resistance mechanisms to CAR T-cell therapy may
57 provide diverse rationales for patient selection or potential strategies.

58 Target antigen evasion has been confirmed as a mechanism for acquired
59 resistance to CAR T-cell therapy.⁷⁻¹⁰ Increasing evidence has suggested that
60 the mechanisms of primary resistance to CAR T-cell therapy involve CAR T-cell
61 defects, including impaired proliferative capacity, an exhaustion phenotype and
62 attenuated T-cell mediated cytotoxicity.^{2,11,12} Nevertheless, intrinsic
63 mechanisms of primary resistance of tumor cells to the treatment remain largely
64 elusive.

65 High-throughput CRISPR/Cas9-based screening is a powerful tool that
66 provides unbiased critical genetic data to exploit for the reasons for resistance
67 to CAR T-cell therapy or to find new biomarkers for stratifying patients. To
68 identify tumor cell-intrinsic factors that determine resistance to CAR T-cell
69 cytotoxicity, we performed unbiased genome-wide CRISPR/Cas9 screening
70 with a coculture model consisting of Nalm6 cells and CD19 CAR T cells. We
71 revealed that CD58, a ligand for the CD2 receptor expressed on T cells,¹³ plays
72 a key role in resistance to CAR T-cell therapy in pre-clinical tests. Disruption of
73 CD58 in tumor cells impaired immunological synapse (IS) formation with CAR
74 T cells, which led to the dysfunction of CAR T cells, including attenuated CAR
75 signal transduction, CAR T-cell expansion and cytotoxicity. Taken together,
76 these findings suggest a potential mechanism for resistance to CAR T-cell
77 therapy.

78

Materials and methods

Additional materials and methods are provided in the supplemental Materials.

CRISPR/Cas9 screening

The process of CRISPR/Cas9 screening has been described in our previous report.¹⁴ Briefly, Nalm6 cells were transfected with lentivirus carrying the Brunello library¹⁵ and cells exhibiting stable lentivirus integrations were selected with puromycin. Transduced Nalm6 cells were cultured with CD19 CAR T cells or control T cells at a 1:50 effector:target (E:T) ratio. Control T or CD19 CAR T cells were added to the culture at a 1:50 E:T ratio every 3 days. The cells were collected using a death cell removal magnetic bead kit (Miltenyi) for genomic DNA analysis on day 15. After removing low-quality reads from the original sequencing data, the reads were mapped to sgRNA sequence, and each sgRNA read was counted to generate a sgRNA count table, in which that data were normalized and used for significance analysis. sgRNA read counts were analysed with the MAGeCK v0.5.7 algorithm. Genes with significantly enriched sgRNAs were identified based on a log₂ fold change (FC) and P value criteria. Hypergeometric distribution statistics were used to identify gene sets that overlapped with candidate genes (log₂ fold change >2 and P < 0.05).

Blocking experiment

Cells were pretreated with blocking mAb against CD58 (clone TS2/9, 8 µg/ml, BioLegend) or CD2 (clone RPA-2.10, 10 µg/ml, eBioscience) or with isotype-matched control mAbs for 30 min. The blocking effect was detected by staining for anti-CD58-PE (BioLegend) or anti-CD2-APC-Cy7 (BioLegend). Tumor cells blocked by anti-CD58 mAbs or CAR T cells blocked by anti-CD2 mAbs were subjected to subsequent experiments, including cytotoxicity assays and degranulation assays, according to the methods described above.

Imaging flow cytometry

109 The sorted CD19 CAR T cells were stained with 0.2 μ M CellTrace Violet dye
110 (Thermo Fisher Scientific) in accordance with the manufacturer's instructions.
111 A total of 1×10^6 WT (mCherry⁺) Nalm6, 1×10^6 CD58^{KO} (GFP⁺) Nalm6 and 1×10^6
112 CD19 CAR T cells (Violet⁺) were cocultured at 37 °C for the indicated times,
113 fixed, permeabilized, and then stained with phalloidin-AF647 (Thermo Fisher
114 Scientific) for detecting F-actin. A total of 1×10^6 events were recorded, and
115 samples were analysed with an ImageStreamX-MKII flow cytometer (Luminex).
116 Image acquisition and data analysis ^{16,17} were performed using IDEAS software
117 version 6.2. The calculation formula for measuring IS is as follows: F-actin
118 enrichment at IS (%) = $100 \times (\text{intensity of phalloidin at IS}) / (\text{intensity of phalloidin-}$
119 $\text{stained CAR T cells})$

120

121 **Xenograft mouse models**

122 A total of 1×10^5 luciferase-positive Nalm6 cells (WT or CD58^{KO}) were
123 intravenously (IV) transplanted into 4 to 6-week-old female NOD-Prkdc-scid-
124 Il2rg-null mice (NPG/Vst, VITALSTAR). Purified CD19 CAR T cells were
125 selected using magnetic beads (Miltenyi Biotec) 3 days post-lentiviral infection.
126 Seven days after Nalm6 cell injection, the mice were IV injected with 1×10^6
127 CD19 CAR T or control T cells in 100 μ l of PBS. (n=6 mice per group). Leukemia
128 burden was monitored once per week by bioluminescence in vivo imaging (BLI)
129 with an IVIS imaging system (PerkinElmer). The average flux (photons per
130 second/area [mm^2]) was used to evaluate the BLI signal. Mouse peripheral
131 blood samples were collected through the orbital sinus and lysed using ACK
132 lysing buffer (Thermo Fisher Scientific). The remaining cells were stained with
133 the indicated fluorochrome-conjugated antibodies. All studies were approved
134 by the Institutional Animal Care and Treatment Committee of the Chinese PLA
135 General Hospital.

136

137 **Statistical analysis**

138 Statistical analyses were conducted using GraphPad Prism 6. Statistical tests

139 were performed using a two-tailed t test, one-way ANOVA test and two-way
140 ANOVA test with Bonferroni correction to compare the significant differences.
141 Survival analysis was analyzed using the log-rank test. Unless otherwise
142 indicated, a p value less than or equal to 0.05 was considered statistically
143 significant for all analyses. All group values are represented as means \pm SD, if
144 not stated otherwise.

145

146 **Results**

147 **CRISPR screening reveals critical regulators that determine resistance to** 148 **CAR T-cell therapy**

149 To systematically identify critical regulators that determine resistance to CAR T-
150 cell therapy in tumor cells, we conducted genome-wide CRISPR/Cas9
151 screening with a coculture model containing Nalm6 cells, CD19⁺ human pre-B
152 ALL cells and CD19 CAR T cells (Figure 1A). The Nalm6 cells were transduced
153 with a lentiviral CRISPR Brunello library targeting ~19,000 genes and then
154 selected under puromycin pressure for 2 days. To better reflect the long-term
155 high tumor burden in vivo, Nalm6 cells were supplemented with CD19 CAR T
156 cells every 3 days for 15 days at a 1:50 E:T ratio.¹⁸ To avoid contamination by
157 the enrichment of single guide RNAs (sgRNAs) that is associated with tumor
158 cell survival but not with CAR T cell therapy, we cocultured Nalm6 cells that had
159 been transduced with the aforementioned CRISPR library with control T cells
160 as the control condition. The composition of the sgRNAs in surviving tumor cells
161 under CAR T-cell or control T-cell treatment conditions was evaluated by
162 Illumina sequencing and analysed by MAGeCK algorithm (supplemental Table
163 1)¹⁹. Our CRISPR screening identified expected candidates among the top 10
164 hits, namely CD19,^{7,8,20} JAK2²¹ and CASP8²² consistent with known
165 mechanisms of resistance to CD19-targeted immunotherapies (Figure 1B).
166 Interestingly, a cluster of membrane protein genes, including CD58, ICAM1,
167 CD81 and ITGA4 were also positively selected (Figure 1C). In order to verify
168 our screening findings, we generated stable KO cell lines of membrane proteins

(CD58, CD81, ICAM1, and ITGA4) in Nalm6 cells by the CRISPR/Cas9 technology (Figure 1D). Growth competition assays were conducted for WT or KO target cell lines with different fluorescence labels in the presence of CAR T cells. The growth competition assays revealed that CD58^{KO} and CD81^{KO} cells conferred progressive enrichment in the presence of CD19 CAR T cells compared with WT cells (Figure 1E-F; supplemental Figure 1A-B). However, ICAM1^{KO} and ITGA4^{KO} cells did not show a significant increase (Figure 1G-H; supplemental Figure 1C-D). We identified that CD81 loss induced disruption of CD19 membrane trafficking (supplemental Figure 2). This finding is similar to previous reports in which downregulation of CD81 has been identified as a mechanism for resistance to CD19-targeted therapy.^{20,23} In the current study, we focused on the role of CD58 in CAR T-cell therapy.

181

182 **Loss of CD58 in tumor cells induces resistance to CAR T-cell therapy**

183 To explore whether CD58-deficient tumor cells mediated resistance to CAR T-
184 cell therapy were limited to CAR design, we also generated distinct CAR T cells
185 including CD20 CAR T, tandem CD19/CD20 CAR T cells²⁴ and CD19.28z CAR
186 T cells from multiple healthy donors and observed that both CD58 loss in Nalm6
187 cells and Raji cells were relatively resistant to CAR T cells (Figure 2A-G;
188 supplemental Figure 3 and supplemental Figure 4A-J). We also found that
189 tumor cells with disruption of CD58 exhibited low sensitivity to CAR T-cell-
190 mediated killing in a cytotoxicity assay (Figure 2H-L; supplemental Figure 2K-
191 M). This effect was recapitulated with an anti-CD58-blocking monoclonal
192 antibody (mAb) (Figure 2M-N). Notably, blockage of CD2 on CAR T cells
193 resulted in impaired CAR-T cell-mediated cytotoxicity (Figure 2O-P). As
194 expected, resistance was not attributed to the downregulation of CD19
195 expression or CD20 expression, as determined by flow cytometry (Figure 2Q-
196 R). Additionally, we observed that knocking out CD58 had no effect on the
197 proliferation or apoptosis of tumor cells (supplemental Figure 5A-C). However,
198 CD58 loss did not protect tumor cells from chemotherapy-mediated killing

(supplemental Figure 5D), implying that CD58 loss in tumor cells may specifically confer resistance to CAR T-cell–mediated killing. Collectively, these findings imply that the CD58-CD2 axis is necessary in cytotoxic killing by CAR T cells and that lack of CD58 in lymphoid cancer cells could induce resistance to CAR T-cell therapy.

204

205 **CD58 disruption in tumor cells impairs CAR T cells**

206 The CD58-CD2 interaction has been reported to be a crucial costimulatory
207 signal for T-cell activation in response to target cells.²⁵ Using TCGA RNA
208 sequencing data and TIMER,²⁶ we found that mRNA levels of CD58 were
209 positively correlated with CD8 T cell infiltration in many human cancer types
210 (supplemental Figure 6A). Besides, we found that the low expression of CD58
211 was associated with the low expression of IFN- γ and TNF- α (supplemental
212 Figure 6B-C), which suggested that the down-regulated expression of CD58 in
213 tumor cells may be related to the dysfunction of T cells. Hence, we wondered
214 whether resistance to CAR T-cell therapy caused by CD58 disruption in cancer
215 cells is due to attenuated CAR T-cell function. We found decreased expansion
216 of CD19 CAR T cells cocultured with CD58^{KO} Nalm6 cells or CD58^{KO} Raji cells
217 (Figure 3A-B). We also observed that lack of CD58 in tumor cells initiated
218 dysfunctional degranulation, as measured by CD107a level (Figure 3B;
219 supplemental Figure 7A). In parallel, adding an anti-CD58-blocking mAb to
220 Nalm6 cell cultures and an anti-CD2-blocking mAb to CD19 CAR T cells
221 cultures significantly inhibited degranulation (Figure 3C-D). Moreover, we found
222 that loss of CD58 in tumor cells led to the reduced secretion of cytokines, such
223 as IL-2, TNF- α and IFN- γ (Figure 3E and supplemental Figure 7B). To further
224 explore the effect of tumor cells with disrupted CD58 on CAR T cells, we sorted
225 CAR T cells cultured with WT or CD58^{KO} tumor cells and then tested their kinetic
226 responses when cocultured with WT tumor cells (Figure 3F). Remarkably, we
227 found that CD19 CAR T cells initially cultured with CD58^{KO} tumor cells exhibited
228 low expansion capacity, a reduced degranulation and impaired ability to kill WT

tumor cells again (Figure 3G-J; supplemental Figure 8A-D). We also noted increased apoptosis in CD19 CAR T cells initially cultured with CD58^{KO} tumor cells, and this increased apoptosis was not driven by FAS or TNFR2 upregulation (Figure 3K; supplemental Figure 8E-F). To investigate the effect of chronic CD58^{KO} tumor cell stimulation on the function of CAR T cells, we established a coculture system in which WT or CD58^{KO} tumor cells were added to a CAR T-cell culture every 72 h (Figure 3L). Repetitive CD58^{KO} tumor cell stimulation attenuated CAR T-cell expansion and reduced CAR T-cell activation as measured by Ki67, CD25 and CD69 level (Figure 3M-O and supplemental Figure 8G-K). Overall, these results suggest that CD58 disruption in cancer cells conferred functional impairment of CAR T cells including reduced CAR T-cell expansion, survival, activation, degranulation, cytotoxicity, cytokine secretion and increased CAR T-cell death, which might be responsible for resistance to CAR T-cell therapy.

243

CD58-deficient tumor cells prevent effective IS formation with CAR T cells and attenuate CAR signaling transduction

The CD2-CD58 interaction is essential for the formation of effective IS, which contribute to sustaining the activation and proliferation of T cells and trigger a series of intracellular signaling pathways in T cells.²⁵ Recent studies have revealed that CAR T cells can initiate cytotoxicity by forming non-classical IS, which has been regarded as important indicators for predicting the effectiveness of CAR T-cell therapy.²⁷⁻²⁹ Therefore, we hypothesized that the inhibition of CAR T-cell function induced by CD58-deficient tumor cells is caused by the ineffective formation of IS and weakened CAR signaling strength. To test this hypothesis, we performed an in vitro conjugation assay.³⁰ Compared to WT cells, CD58^{KO} Nalm6 cells formed significantly fewer conjugates with CAR-expressing Jurkat cells or CAR T cells (Figure 4A and supplemental Figure 9).

258

259 Next, we used high-throughput imaging flow cytometry (ImageStream) to
 260 evaluate the stability of IS (Figure 4B). CD58^{KO} Nalm6 cells formed IS
 261 structures with potentially disadvantageous cytoskeletal properties, as
 262 measured by F-actin intensity and enrichment at the IS (Figure 4C-D), implying
 263 that CD58^{KO} Nalm6 cells prevented effective IS formation with CAR T cells.
 264 Considering that the production of CAR T cells requires the activation of anti-
 265 CD3 antibody, the background phosphorylation level so high that we could not
 266 detect differences between groups. We observed that the phosphorylation of
 267 CD3ζ-CAR, LCK or ZAP70 in CAR-expressing Jurkat cells stimulated with
 268 CD58^{KO} Nalm6 cells was inhibited compared to that stimulated with WT Nalm6
 269 cells (Figure 4E). Of note, an anti-CD2 antibody can activate CAR T cells by
 270 detecting the expression of CD25 in CAR T cells (supplemental Figure 10 A).
 271 However, CD58 loss in tumor cells did not show increased sensitivity to CAR T
 272 cells after the addition of an anti-CD2 antibody (supplemental Figure 10 B),
 273 indicating the stable IS formed by CD58 on tumor cells is necessary for CAR T
 274 cells to successfully kill tumor cells.
 275
 276 To decipher the underlying molecular programs accounting for CD58-deficient
 277 tumor-mediated CAR T-cell dysfunction, we leveraged the transcriptional
 278 profiles of CD19 CAR T cells cocultured with WT Nalm6 cells or CD58^{KO} Nalm6
 279 cells. We observed differentially expressed genes in CD19 CAR T cells
 280 stimulated with WT Nalm6 cells or CD58^{KO} Nalm6 cells (supplemental Figure
 281 11A). A gene enrichment analysis of these differentially expressed genes
 282 revealed that these genes were significantly enriched in regulation of cell
 283 adhesion, T-cell activation, cytokine related signaling and cell proliferation
 284 (Figure 4F; supplemental Figure 11B-C; supplemental Table 2). More
 285 specifically, CD19 CAR T cells cocultured with CD58^{KO} Nalm6 cells showed
 286 marked downregulation of genes associated with activation (RIPOR2, IL1A,
 287 RUNX1, NFKB2, SDC4 and TNFRSF4),³¹⁻³⁵ and significantly differentially
 288 expressed genes associated with T-cell differentiation (CXCR4, CCR7, TOX,

LGALS3 and XBP1).³⁶⁻³⁸ In addition, we found that the expression of a cluster of cytokine genes (IFNG, TNF, IL17F, IL13, CCL3L3 and CCL5) were decreased in CAR T cells cocultured with CD58^{KO} Nalm6 cells (Figure 4G). Taken together, these findings indicates that CD58^{KO} tumor cells and CAR T cells forms inefficient IS, which drives a reduction in CAR T-cell activation, resulting in CAR T-cell dysfunction.

Loss of CD58 in tumor cells exhibits resistance to CAR T-cell therapy in vivo

To evaluate the effect of CD58 knockout in tumor cells on the anti-tumor ability of CAR T-cell therapy in mouse xenograft models, we examined the tumor-suppressive ability of equal amounts of CAR T cells in mice transplanted with WT tumor cells or CD58^{KO} tumor cells (Figure 5A). Consistent with our in vitro observations, the CD19 CAR T cells in CD58^{KO} Nalm6 cell-bearing mice showed low tumor clearance capacity (Figure 5B-C). Moreover, xenograft mice with CD58^{KO} Nalm6 cell transplants exhibited a survival disadvantage compared to xenograft mice with WT Nalm6 cell transplants (Figure 5D). Consistently, the expansion of CAR T cells in peripheral blood in CD58^{KO} tumor-bearing mice was significantly lower than that in WT tumor-bearing mice (Figure 5E). Besides, we found that loss of CD58 in tumor cells suppressed activation of CAR T cells, as measured by CD25 level (Figure 5F). CAR T cells in the CD58^{KO} tumor group secreted less cytokines than those in the WT tumor group (Figure 5G). These results indicate that loss of CD58 in tumor cells results in reduced sensitivity to CD19 CAR T-cell therapy in vivo.

Discussion

Resistance to CAR T-cell therapy is a primary obstacle to its broader therapeutic use.³⁹ Performing unbiased CRISPR/Cas9 screening with the Nalm6 cells, CD19⁺ human ALL cell line, we revealed several genetic perturbations potentially capable of mediating resistance to CAR T-cell therapy.

319 In addition to antigen loss and T-cell dysfunction, tumor-intrinsic resistance
320 mechanisms, such as impaired death receptor signaling and NOXA, have been
321 recently reported.^{18,22,40} In the present study, we identified a potential
322 mechanism of tumor-intrinsic resistance to CAR T-cell therapy mediated by the
323 loss of CD58 in tumor cells.

324
325 CD58 is a member of the immunoglobulin superfamily and is a ligand for the
326 costimulatory molecule CD2 expressed in T cells.⁴¹ Disruption of the CD58-CD2
327 axis by blocking antibodies results in decreased T cell activation, reduced IFN-
328 γ secretion and reduced cytotoxicity.^{42,43} Several reports have shown that loss
329 of CD58 in tumor cells is an unfavorable prognostic factor and a frequent
330 genetic abnormality in patients with hematologic malignancies.^{44,45} On the basis
331 of CRISPR/Cas9 screening, a recent study has revealed that CD58 loss can
332 confer immune evasion in tumor-infiltrating lymphocyte-mediated killing and
333 that CD58 expression is downregulated in tumors of melanoma patients with
334 resistance to immune checkpoint inhibitors.⁴⁶ Likewise, in another study which
335 CRISPR/Cas9 screening was implemented showed that CD58 deletion caused
336 Nalm6 cell escape from natural killer (NK) cell-mediated killing.⁴⁷ These data
337 suggest that abnormal CD58 expression in tumor cells may confer general
338 resistance to various immunotherapies and that further investigation is needed
339 in future studies.

340
341 CD58 is essential for the formation of stable IS, maintenance of T-cell activation,
342 T-cell survival and T cell-mediated killing.^{25,48} However, the effect of CD58
343 expression in tumor cells on CAR T-cell therapy remains unknown. In this study,
344 we observed that CD58 knockout in two B-lymphoid cell lines showed
345 significantly less sensitive to a series of CAR T cells, including CD19 CAR T,
346 CD20 CAR T, and tandem CD19/20 CAR T cells. In addition, we found that the
347 loss of CD58 in tumor cells triggered impaired CAR T cells, which resulted in
348 decreased CAR T-cell proliferation, degranulation, cytokine secretion, cytotoxic

effects and increased cell death. Even if the structure of IS formed by CAR T cells and target cells is saliently distinct from that of classical IS, but an increasing number of studies demonstrated that the IS formed by CAR T cells plays an important role in driving the cytotoxic function of CAR T cells.^{27-29,49,50} In this study, we observed that CD58 loss in tumor cells prevented effective IS formation with CAR T cells, as measured by the intensity and enrichment of F-actin, a key component in IS.^{16,51} Furthermore, we found that CAR T cells saliently attenuated CAR signaling and CAR T-cell activation stimulation by CD58-deficient tumor cells. These results may shed light on the reasons that loss of CD58 in tumor cells induces resistance to CAR T-cell therapy.

Unfortunately, we were unable to provide clinical relevance of CD58 protein levels to CAR T cell therapy in hematologic malignancies. Factually, we detected CD58 protein levels in tumor specimens from 34 B-cell lymphoma patients before infusions of tandem CD19/20 CAR T cells by immunohistochemistry^{24,52}. Unexpectedly, we found only two patients with low CD58 expression (data not shown), which is totally distinct from the 60% DLBCL patients of CD58 protein downregulation reported by others^{53,54} in western population. In addition, we noted a large difference of CD58 mutation frequency in DLBCL patients between Chinese population (around 5%-10% mutation rate)^{44,55} and western population (>20% mutation rate).^{53,54} Although the two patients with CD58 low expression had poor response in our tandem CD19/20 CAR T-cell clinical trial, few sample number limited further comparative analysis. We preliminarily speculate that the expression of CD58 may be affected by racial disparities, CD58 loss or downregulation was not a mainly contributing factor for resistance to CAR T-cell therapy, just a low-probability event in Chinese DLBCL patients.

Strategies to overcome tumor resistance to CAR T-cell therapy caused by CD58 loss remains to be further explored. A recent study illuminated that

bypassing CD58 loss in tumor cells using a novel CAR T-cell construct integrating CD2 costimulatory domains with CAR molecules may be a potential therapeutic strategy.⁵⁶ CD58 is regulated by both genetic and non-genetic factors.⁵⁷ A previous study suggested that an EZH2 inhibitors can restore epigenetically silenced CD58 expression on the surface of lymphoma cells, which in turn enhance IFN- γ secretion by T/NK cells.⁴³ Reversing the functional downregulation of CD58 in tumor cells using drugs such as epigenetic modulators may contribute to novel combinatorial treatment strategies that can improve clinical responses to CAR T-cell therapy.

Overall, our findings emphasize a potential molecular mechanism determining the resistance of B-cell malignancies to CAR T-cell therapy. Our observations suggest that CD58 may be a clinically predictive biomarker for evaluating response to CAR T-cell therapy in hematologic malignancies, and therefore, targeting CD58 may be a novel therapeutic avenue to enhance the sensitivity or overcome resistance to CAR T-cell therapy.

Acknowledgements

This work was supported in part by the National Natural Science Foundation of China (Nos. 81830002, 82150108 and 31991171) and Translational Research Grant of NCRCH (2021WWC04).

Author contributions

X.Y., D.C., Y.W., Z.W. and W.H. designed the study. X.Y., D.C., X.M. and Y.W. performed the experiments. Y.W., Y.G., J.W., Q.Z., Y.L., Y.Y. and C.T. assisted with the experiments. X.Y. and D.C., Z.W., and W.H. analysed the data and wrote the original manuscript. All authors reviewed the manuscript.

Disclosure of conflicts of interest

The authors declare no competing interests.

409 **Figure legends**

410 **Figure 1. Use of CRISPR/Cas9 screening to study intrinsic tumor**
411 **resistance mechanisms to CAR T cells**

412 (A) Schematic showing the CRISPR/Cas9 screening process. (B) The 10 genes
413 with most significant sgRNA enrichment. (C) Log 2 fold change (FC) of
414 normalized counts of each sgRNA targeting CD58, CD81, ICAM1 or ITGA4 in
415 the screening. (D) Efficacy of CD58, CD81, ICAM1 or ITGA4 KO in Nalm6 cells.
416 (E-H) GFP-labeled indicated KO cells and mCherry-labeled WT cells were
417 mixed at an approximately 1:1 ratio and co-cultured with control T or CAR T
418 cells. The KO (GFP⁺)/WT (mCherry⁺) ratio was calculated over time.
419 CD58^{KO}/WT Nalm6 ratio (E), CD81^{KO}/WT Nalm6 ratio (F), ICAM1^{KO}/WT Nalm6
420 ratio (G) and ITGA4^{KO}/WT Nalm6 ratio (H) in growth competition assay. KO cell
421 lines referred to sgRNA-1 targeting the indicated genes in (E-H). A mixture of
422 cells were cocultured with control T or CD19 CAR T cells at a 1:20 E:T ratio of
423 (n=3). Statistical comparisons were performed using a two-way ANOVA test
424 with multiple comparisons. The values are shown as the means \pm SD. ns, not
425 significant ($p>0.05$); * $p<0.05$, ** $p<0.01$, *** $p<0.001$.

426

427 **Figure 2. Role of CD58 in resistance to CAR T-cell-mediated killing**

428 (A-C) CD58^{KO}/WT Nalm6 cell ratio in growth competition assays. CD58^{KO}
429 Nalm6 cells referred to sgCD58-2 Nalm6 cells. (A) A mixture of Nalm6 cells
430 were cocultured with control T cells or CD20 CAR T cells at a 1:1 E:T ratio (n=3).
431 (B) A mixture of Nalm6 cells were cocultured with control T cells or tandem
432 CD19/20 CAR T cells at a 1:20 E:T ratio (n=3). (C) A mixture of Nalm6 cells
433 were cocultured with control T cells or CD19.28z CAR T cells at a 1:20 E:T ratio
434 (n=4). (D-G) CD58^{KO}/WT Raji cell ratio in a growth competition assay. CD58^{KO}
435 Raji cells referred to sgCD58-2 Raji cells. (D) A mixture of Raji cells were
436 cocultured with control T cells or CD19 CAR T cells at a 1:20 E:T ratio (n=3).
437 (E) A mixture of Raji cells were cocultured with control T cells or CD20 CAR T
438 cells at a 1:20 E: T ratio (n=3). (F) A mixture of Raji cells were cocultured with

control T cells or CD19/20 CAR T cells at a 1:20 E: T ratio (n=4). (G) A mixture of Raji cells were cocultured with control T cells or CD19.28z CAR T cells at a 1:20 E: T ratio (n=4). (H) Cytotoxic analysis of WT and CD58^{KO} Nalm6 cells cocultured with CD19 CAR T cells at indicated E:T ratios for 24 h (n=3). (I) Cytotoxic analysis of WT and CD58^{KO} Nalm6 cells cocultured with CD19/20 CAR T cells at indicated E:T ratios for 24 h (n=4). (J) Cytotoxic analysis of WT and CD58^{KO} Nalm6 cells cocultured with CD19.28z CAR T cells at indicated E:T ratios for 24 h (n=4). (K) Cytotoxic analysis of WT and CD58^{KO} Raji cells cocultured with CD19 CAR T cells at indicated E:T ratios for 24 h (n=4). (L) Cytotoxic analysis of WT and CD58^{KO} Raji cells cocultured with CD19/20 CAR T cells at indicated E:T ratios for 24 h (n=4). (M) FACS histogram showing the CD58 level in Nalm6 or Raji cell lines pretreated with control or blocking anti-CD58 monoclonal antibodies (mAbs) for 30 min. (N) Cytotoxic analysis of Nalm6 or Raji cells pretreated with control or anti-CD58 blocking mAbs and cocultured with CD19 CAR T cells for 24 h at a 1:20 E:T ratio (n=3). (O) Representative FACS histogram showing the CD2 level in CD19 CAR T cells pretreated with control or anti-CD2 blocking mAbs for 30 min. (P) Cytotoxicity analysis of Nalm6 or Raji cells cocultured with control or anti-CD2 mAb-blocked CD19 CAR T cells at a 1:20 E:T ratio for 24 h (n=3). (Q) Representative FACS plot showing the level of CD19 expression in WT and CD58^{KO} cell lines. (R) Representative FACS plot showing the level of CD20 expression in WT and CD58^{KO} cell lines. Significance was assessed using a two-way ANOVA test with multiple comparisons (A-L). Statistical comparisons were performed using a two-tailed unpaired t test (N and P). The values are shown as the means \pm SD. ns, not significant ($p>0.05$); * $p<0.05$, ** $p<0.01$, *** $p<0.001$.

Figure 3. Loss of CD58 in tumor cells gives rise to CAR T-cell dysfunction

(A) Expansion of CD19 CAR T cells after coculturing with WT or CD58^{KO} Nalm6 or Raji cells at a 1:1 E:T ratio (n=3). (B) FACS-based measurement of CD107a expression in CD19 CAR T cells stimulated by WT or CD58^{KO} Nalm6 or Raji

469 cells (n=4). (C) FACS-based measurement of CD107a expression in CD19
 470 CAR T cells stimulated with Nalm6 or Raji cells pretreated with control or anti-
 471 CD58-blocking monoclonal antibodies (mAbs) (n=4). (D) FACS-based
 472 measurement of CD107a expression in CD19 CAR T cells pretreated with
 473 control or anti-CD2 blocking mAbs after stimulation with Nalm6 cells or Raji
 474 cells (n=4). (E) FACS-based quantification of intracellular IL-2, IFN- γ and TNF-
 475 α expression in CD19 CAR T cells stimulated with WT or CD58^{KO} Nalm6 cells
 476 (n=4) or Raji cells (n=5) at a 1:1 E:T ratio for 8 h. (F) Schematic showing the
 477 functional assessment study. CD19 CAR T cells and WT or CD58^{KO} Nalm6 cells
 478 were initially cocultured at an E: T ratio of 1:1 for 3 days (first coculture). CD19
 479 CAR T cells were sorted by the PE magnetic beads method based on CAR
 480 staining in first co-culture and then cocultured again with WT Nalm6 cells at an
 481 E:T ratio of 1:1 for 24 h and 48 h (secondary coculture). Expansion (G) and
 482 Ki67 expression (H) of CD19 CAR T cells after 24 h and 48 h in secondary
 483 coculture (n=3). (I) CD19 CAR T cells were sorted in first coculture and then
 484 cocultured again with WT Nalm6 cells at an E:T ratio of 1:1 to test the
 485 degranulation (CD107a expression) of CAR T cells for 0.5 h or 1 h (n=4). (J)
 486 Survival of WT Nalm6 cells after 24 h and 48 h in secondary coculture (n=3).
 487 (K) Representative FACS plots and quantification of Annexin V expression of
 488 CD19 CAR T cells after 24 h and 48 h in secondary coculture (n=3). (L) Pattern
 489 of repeated antigen stimulation in vitro. ("↓" represents the time point when WT
 490 or CD58^{KO} Nalm6 or Raji cells were added). (M) CD19 CAR T cell-expansion
 491 after repeated stimulation with WT or CD58^{KO} Nalm6 cells. CD25 (N) and CD69
 492 expression (O) in CD19 CAR T cells after repeated stimulation with WT or
 493 CD58^{KO} Nalm6 cells (n=3). Statistical comparisons were performed using a two-
 494 tailed unpaired t test (C, D). Statistical comparisons were performed using a
 495 one-way ANOVA test (B, E). Significance was assessed using a two-way
 496 ANOVA test with multiple comparisons (A, G-K and M-O). The values are shown
 497 as the means \pm SD. ns, not significant (p>0.05); *p<0.05, **p < 0.01, *** p<
 498 0.001.

Figure 4. Knockout of CD58 in tumor cells forms ineffective immunological synapse (IS) with CAR T cells and attenuates CAR signaling.

(A) CD19 CAR T cells were stained with CellTrace Violet dye and incubated with WT Nalm6(mCherry+) and CD58^{KO} (GFP+) Nalm6 cells for 10 min or 30 min. Representative FACS and bar plots(gating from Violet⁺ cells) representing the quantification of conjugates formed by WT or CD58^{KO} with CAR T cells (n=3). (B) CD19 CAR T cells prestained with CellTrace Violet dye were cocultured with WT (mCherry+) or CD58^{KO} (GFP+) Nalm6 cells for 10 min or 30 min. After incubation, the cells were analysed for the expression of CellTrace Violet, GFP, mCherry and phalloidin (AF647) using ImageStream. Phalloidin was used to stain F-actin. The gating strategy used for the identification of IS and a representative image of an IS are shown. The white arrow points to an IS. (C) Median fluorescence intensity (MFI) of phalloidin at IS (n=3). (D) F-actin enrichment at IS with WT or CD58^{KO} is reported as percent protein (n=3). (E) Proximal signaling events of CAR-expressing Jurkat cells upon stimulation with WT or CD58^{KO} Nalm6 cells. Similar results were obtained from three independent biological experiments. (F) Selected pathways of Gene Ontology (GO) enrichment analysis in the biological process category of differentially expressed genes in CD19 CAR T cells sorted by flow cytometry 3 days after stimulation with WT or CD58^{KO} Nalm6 cells (n = 2 different peripheral blood mononuclear cell [PBMC] donors). (G) Heatmap showing select differentially expressed genes related to T-cell activation, T-cell differentiation and cytokines in CD19 CAR T cells after 3 days stimulation with WT or CD58^{KO} Nalm6 cells (n = 2 different PBMC donors). Statistical comparisons were performed using a two-way ANOVA test with multiple comparisons. The values are shown as the means \pm SD. ns, not significant (p>0.05); *p<0.05, **p < 0.01, *** p< 0.001.

527

Figure 5. CD58-deficient tumors show decreased sensitivity to CAR T-cell

528

therapy in mouse xenograft model

(A) Schematic showing the generation of xenograft mouse models. NPG mice (n=6/group) were injected intravenously (IV) with 1×10^5 WT or CD58^{KO} Nalm6-luk cells 7 days after a single IV injection of 1×10^6 control T cells or CD19 CAR T cells. Tumor burden was monitored every 7 days with bioluminescence in vivo imaging (BLI) with an IVIS imaging system. (B) IVIS-obtained images showing tumor burden; BLI was performed at the indicated time points. (C) Average radiance measurement at the indicated time points (n=6). (D) Mouse survival was monitored and recorded (n=6/group). (E) T-cell persistence in peripheral blood on days 7 and 14 (n=6). (F) FACS-based measurement of CD25 expression in CD19 CAR T cells in peripheral blood on days 7 (n=6). (G) Cytokines in peripheral blood at 7 days after CAR T cell infusion were measured by ELISAs (n=6). Significance was assessed using two-way ANOVA with multiple comparisons (C and E). Log-rank tests were performed to assess the significance of difference (D). Statistical comparisons were performed using a two-tailed unpaired t test (F). Statistical comparisons were performed using a one-way ANOVA test (G). The values are shown as the means \pm SD of 6 mice per group. For B-G, the results were from one of three independent experiments. ns, not significant ($p > 0.05$); * $p < 0.05$, ** $p < 0.01$, *** $p < 0.001$.

References

1. Lesch S, Benmeharek MR, Cadilha BL, et al. Determinants of response and resistance to CAR T cell therapy. *Semin Cancer Biol.* 2020;65:80-90.
2. Schuster SJ, Bishop MR, Tam CS, et al. Tisagenlecleucel in Adult Relapsed or Refractory Diffuse Large B-Cell Lymphoma. *N Engl J Med.* 2019;380(1):45-56.
3. Locke FL, Ghobadi A, Jacobson CA, et al. Long-term safety and activity of axicabtagene ciloleucel in refractory large B-cell lymphoma (ZUMA-1): a single-arm, multicentre, phase 1-2 trial. *Lancet Oncol.* 2019;20(1):31-42.
4. Park JH, Riviere I, Gonen M, et al. Long-Term Follow-up of CD19 CAR

559 Therapy in Acute Lymphoblastic Leukemia. *N Engl J Med.* 2018;378(5):449-
560 459.

561 5. Maude SL, Laetsch TW, Buechner J, et al. Tisagenlecleucel in Children and
562 Young Adults with B-Cell Lymphoblastic Leukemia. *N Engl J Med.*
563 2018;378(5):439-448.

564 6. Shah NN, Fry TJ. Mechanisms of resistance to CAR T cell therapy. *Nat Rev*
565 *Clin Oncol.* 2019;16(6):372-385.

566 7. Orlando EJ, Han X, Tribouley C, et al. Genetic mechanisms of target
567 antigen loss in CAR19 therapy of acute lymphoblastic leukemia. *Nat Med.*
568 2018;24(10):1504-1506.

569 8. Sotillo E, Barrett DM, Black KL, et al. Convergence of Acquired Mutations
570 and Alternative Splicing of CD19 Enables Resistance to CART-19
571 Immunotherapy. *Cancer Discov.* 2015;5(12):1282-1295.

572 9. Fry TJ, Shah NN, Orentas RJ, et al. CD22-targeted CAR T cells induce
573 remission in B-ALL that is naive or resistant to CD19-targeted CAR
574 immunotherapy. *Nat Med.* 2018;24(1):20-28.

575 10. Plaks V, Rossi JM, Chou J, et al. CD19 target evasion as a mechanism of
576 relapse in large B-cell lymphoma treated with axicabtagene ciloleucel. *Blood.*
577 2021.

578 11. Turtle CJ, Hanafi LA, Berger C, et al. CD19 CAR-T cells of defined
579 CD4+:CD8+ composition in adult B cell ALL patients. *J Clin Invest.*
580 2016;126(6):2123-2138.

581 12. Fraietta JA, Lacey SF, Orlando EJ, et al. Determinants of response and
582 resistance to CD19 chimeric antigen receptor (CAR) T cell therapy of chronic
583 lymphocytic leukemia. *Nat Med.* 2018;24(5):563-571.

584 13. Wang JH, Smolyar A, Tan K, et al. Structure of a heterophilic adhesion
585 complex between the human CD2 and CD58 (LFA-3) counterreceptors. *Cell.*
586 1999;97(6):791-803.

587 14. Savoldo B, Ramos CA, Liu E, et al. CD28 costimulation improves
588 expansion and persistence of chimeric antigen receptor-modified T cells in

- lymphoma patients. *J Clin Invest.* 2011;121(5):1822-1826.
15. Doench JG, Fusi N, Sullender M, et al. Optimized sgRNA design to maximize activity and minimize off-target effects of CRISPR-Cas9. *Nat Biotechnol.* 2016;34(2):184-191.
16. Wabnitz G, Kirchgessner H, Samstag Y. Qualitative and Quantitative Analysis of the Immune Synapse in the Human System Using Imaging Flow Cytometry. *J Vis Exp.* 2019(143).
17. Balta E, Stopp J, Castelletti L, Kirchgessner H, Samstag Y, Wabnitz GH. Qualitative and quantitative analysis of PMN/T-cell interactions by InFlow and super-resolution microscopy. *Methods.* 2017;112:25-38.
18. Yan X, Chen D, Wang Y, et al. Identification of NOXA as a pivotal regulator of resistance to CAR T-cell therapy in B-cell malignancies. *Signal Transduct Target Ther.* 2022;7(1):98.
19. Li W, Koster J, Xu H, et al. Quality control, modeling, and visualization of CRISPR screens with MAGeCK-VISPR. *Genome Biol.* 2015;16:281.
20. Zhao Y, Aldoss I, Qu C, et al. Tumor-intrinsic and -extrinsic determinants of response to blinatumomab in adults with B-ALL. *Blood.* 2021;137(4):471-484.
21. Arenas EJ, Martinez-Sabadell A, Rius Ruiz I, et al. Acquired cancer cell resistance to T cell bispecific antibodies and CAR T targeting HER2 through JAK2 down-modulation. *Nat Commun.* 2021;12(1):1237.
22. Singh N, Lee YG, Shestova O, et al. Impaired death receptor signaling in leukemia causes antigen-independent resistance by inducing CAR T cell dysfunction. *Cancer Discov.* 2020.
23. Braig F, Brandt A, Goebeler M, et al. Resistance to anti-CD19/CD3 BiTE in acute lymphoblastic leukemia may be mediated by disrupted CD19 membrane trafficking. *Blood.* 2017;129(1):100-104.
24. Tong C, Zhang Y, Liu Y, et al. Optimized tandem CD19/CD20 CAR-engineered T cells in refractory/relapsed B-cell lymphoma. *Blood.* 2020;136(14):1632-1644.
25. Demetriou P, Abu-Shah E, Valvo S, et al. A dynamic CD2-rich compartment

619 at the outer edge of the immunological synapse boosts and integrates signals.
620 *Nat Immunol.* 2020;21(10):1232-1243.

621 26. Li B, Severson E, Pignon JC, et al. Comprehensive analyses of tumor
622 immunity: implications for cancer immunotherapy. *Genome Biol.*
623 2016;17(1):174.

624 27. Liu D, Badeti S, Dotti G, et al. The Role of Immunological Synapse in
625 Predicting the Efficacy of Chimeric Antigen Receptor (CAR) Immunotherapy.
626 *Cell Commun Signal.* 2020;18(1):134.

627 28. Xiong W, Chen Y, Kang X, et al. Immunological Synapse Predicts
628 Effectiveness of Chimeric Antigen Receptor Cells. *Mol Ther.* 2018;26(4):963-
629 975.

630 29. Davenport AJ, Cross RS, Watson KA, et al. Chimeric antigen receptor T
631 cells form nonclassical and potent immune synapses driving rapid cytotoxicity.
632 *Proc Natl Acad Sci U S A.* 2018;115(9):E2068-E2076.

633 30. Chu C, Wang Y, Zhang X, et al. SAP-regulated T Cell-APC adhesion and
634 ligation-dependent and -independent Ly108-CD3zeta interactions. *J Immunol.*
635 2014;193(8):3860-3871.

636 31. Fu Y, Lin Q, Zhang Z, Zhang L. Therapeutic strategies for the costimulatory
637 molecule OX40 in T-cell-mediated immunity. *Acta Pharm Sin B.*
638 2020;10(3):414-433.

639 32. Wong WF, Looi CY, Kon S, et al. T-cell receptor signaling induces proximal
640 Runx1 transactivation via a calcineurin-NFAT pathway. *Eur J Immunol.*
641 2014;44(3):894-904.

642 33. Rougerie P, Largeteau Q, Megrelis L, et al. Fam65b is a new transcriptional
643 target of FOXO1 that regulates RhoA signaling for T lymphocyte migration. *J*
644 *Immunol.* 2013;190(2):748-755.

645 34. Elfenbein A, Simons M. Syndecan-4 signaling at a glance. *J Cell Sci.*
646 2013;126(Pt 17):3799-3804.

647 35. Vallabhapurapu S, Karin M. Regulation and function of NF-kappaB
648 transcription factors in the immune system. *Annu Rev Immunol.* 2009;27:693-

649 733.

650 36. Scott AC, Dundar F, Zumbo P, et al. TOX is a critical regulator of tumour-
651 specific T cell differentiation. *Nature*. 2019;571(7764):270-274.

652 37. Khan AB, Carpenter B, Santos ESP, et al. Redirection to the bone marrow
653 improves T cell persistence and antitumor functions. *J Clin Invest*.
654 2018;128(5):2010-2024.

655 38. Pramanik J, Chen X, Kar G, et al. Genome-wide analyses reveal the IRE1a-
656 XBP1 pathway promotes T helper cell differentiation by resolving secretory
657 stress and accelerating proliferation. *Genome Med*. 2018;10(1):76.

658 39. Singh N, Orlando E, Xu J, et al. Mechanisms of resistance to CAR T cell
659 therapies. *Semin Cancer Biol*. 2020;65:91-98.

660 40. Dufva O, Koski J, Maliniemi P, et al. Integrated drug profiling and CRISPR
661 screening identify essential pathways for CAR T-cell cytotoxicity. *Blood*.
662 2020;135(9):597-609.

663 41. Binder C, Cvetkovski F, Sellberg F, et al. CD2 Immunobiology. *Front*
664 *Immunol*. 2020;11:1090.

665 42. Zhang Y, Liu Q, Yang S, Liao Q. CD58 Immunobiology at a Glance. *Front*
666 *Immunol*. 2021;12:705260.

667 43. Otsuka Y, Nishikori M, Arima H, et al. EZH2 inhibitors restore epigenetically
668 silenced CD58 expression in B-cell lymphomas. *Mol Immunol*. 2020;119:35-45.

669 44. Cao Y, Zhu T, Zhang P, et al. Mutations or copy number losses of CD58 and
670 TP53 genes in diffuse large B cell lymphoma are independent unfavorable
671 prognostic factors. *Oncotarget*. 2016;7(50):83294-83307.

672 45. Archimbaud E, Thomas X, Campos L, Magaud JP, Dore JF, Fiere D.
673 Expression of surface adhesion molecules CD54 (ICAM-1) and CD58 (LFA-3)
674 in adult acute leukemia: relationship with initial characteristics and prognosis.
675 *Leukemia*. 1992;6(4):265-271.

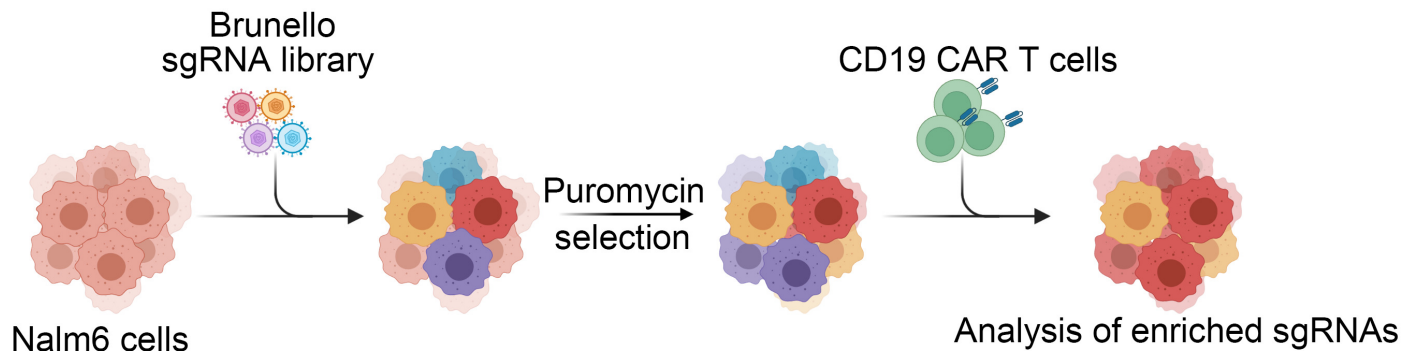
676 46. Frangieh CJ, Melms JC, Thakore PI, et al. Multimodal pooled Perturb-CITE-
677 seq screens in patient models define mechanisms of cancer immune evasion.
678 *Nat Genet*. 2021;53(3):332-341.

- 679 47. Pech MF, Fong LE, Villalta JE, et al. Systematic identification of cancer cell
680 vulnerabilities to natural killer cell-mediated immune surveillance. *Elife*. 2019;8.
- 681 48. Daniel PT, Scholz C, Essmann F, Westermann J, Pezzutto A, Dorken B.
682 CD95/Fas-triggered apoptosis of activated T lymphocytes is prevented by
683 dendritic cells through a CD58-dependent mechanism. *Exp Hematol*.
684 1999;27(9):1402-1408.
- 685 49. Strohl WR, Naso M. Bispecific T-Cell Redirection versus Chimeric Antigen
686 Receptor (CAR)-T Cells as Approaches to Kill Cancer Cells. *Antibodies (Basel)*.
687 2019;8(3).
- 688 50. Fousek K, Watanabe J, Joseph SK, et al. CAR T-cells that target acute B-
689 lineage leukemia irrespective of CD19 expression. *Leukemia*. 2021;35(1):75-
690 89.
- 691 51. Mukherjee M, Mace EM, Carisey AF, Ahmed N, Orange JS. Quantitative
692 Imaging Approaches to Study the CAR Immunological Synapse. *Mol Ther*.
693 2017;25(8):1757-1768.
- 694 52. Zhang Y, Wang Y, Liu Y, et al. Long-term activity of tandem CD19/CD20
695 CAR therapy in refractory/relapsed B-cell lymphoma: a single-arm, phase 1-2
696 trial. *Leukemia*. 2022;36(1):189-196.
- 697 53. Testoni M, Zucca E, Young KH, Bertoni F. Genetic lesions in diffuse large
698 B-cell lymphomas. *Annals of Oncology*. 2015;26(6):1069-1080.
- 699 54. Pasqualucci L, Trifonov V, Fabbri G, et al. Analysis of the coding genome
700 of diffuse large B-cell lymphoma. *Nat Genet*. 2011;43(9):830-837.
- 701 55. Huo YJ, Xu PP, Fu D, et al. Molecular heterogeneity of CD30+ diffuse large
702 B-cell lymphoma with prognostic significance and therapeutic implication. *Blood*
703 *Cancer J*. 2022;12(3):48.
- 704 56. Majzner RG, Frank MJ, Mount C, et al. CD58 aberrations limit durable
705 responses to CD19 CAR in large B cell lymphoma patients treated with
706 axicabtagene ciloleucel but can be overcome through novel CAR engineering.
707 *Blood*. 2020;136:53-54.
- 708 57. Challa-Malladi M, Lieu YK, Califano O, et al. Combined genetic inactivation

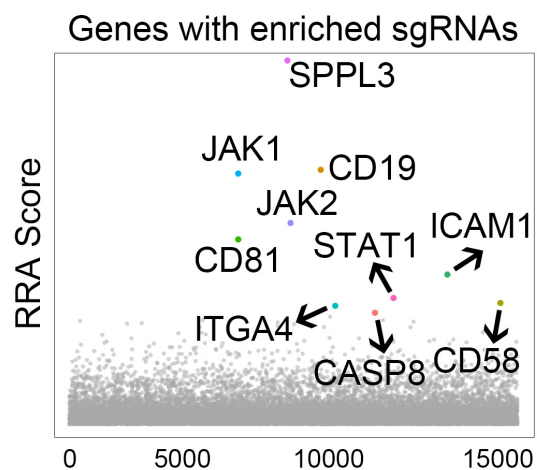
709 of beta2-Microglobulin and CD58 reveals frequent escape from immune
710 recognition in diffuse large B cell lymphoma. *Cancer Cell*. 2011;20(6):728-740.

Figure 1

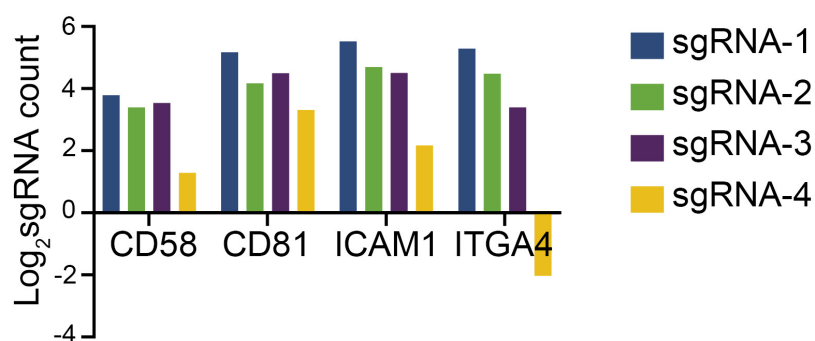
A



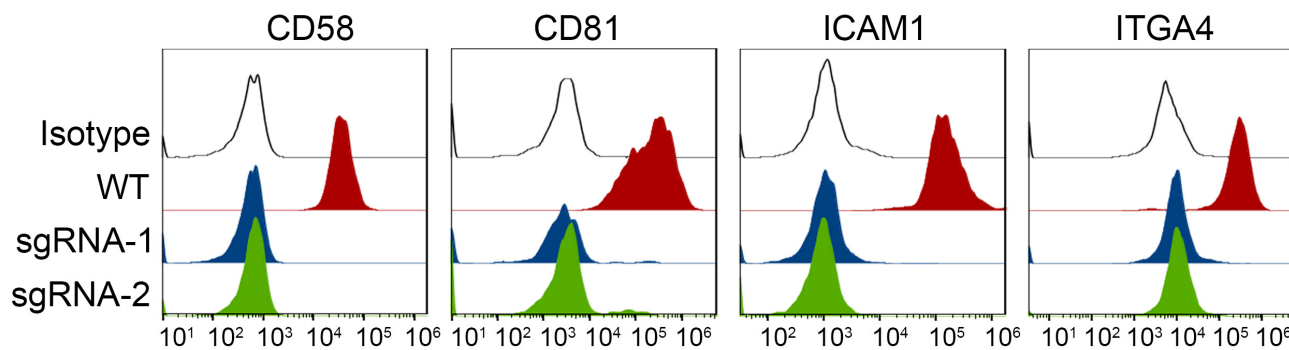
B



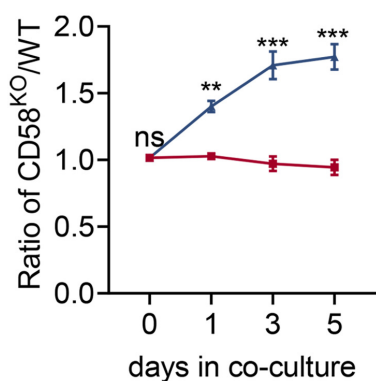
C



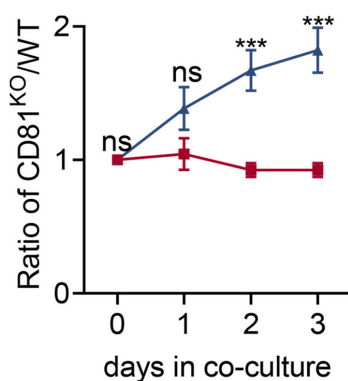
D



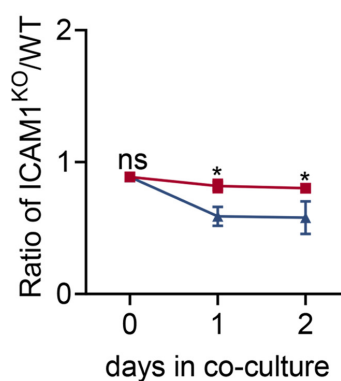
E



F



G



H

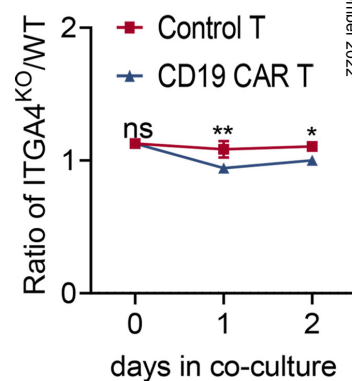


Figure 2

Figure 2

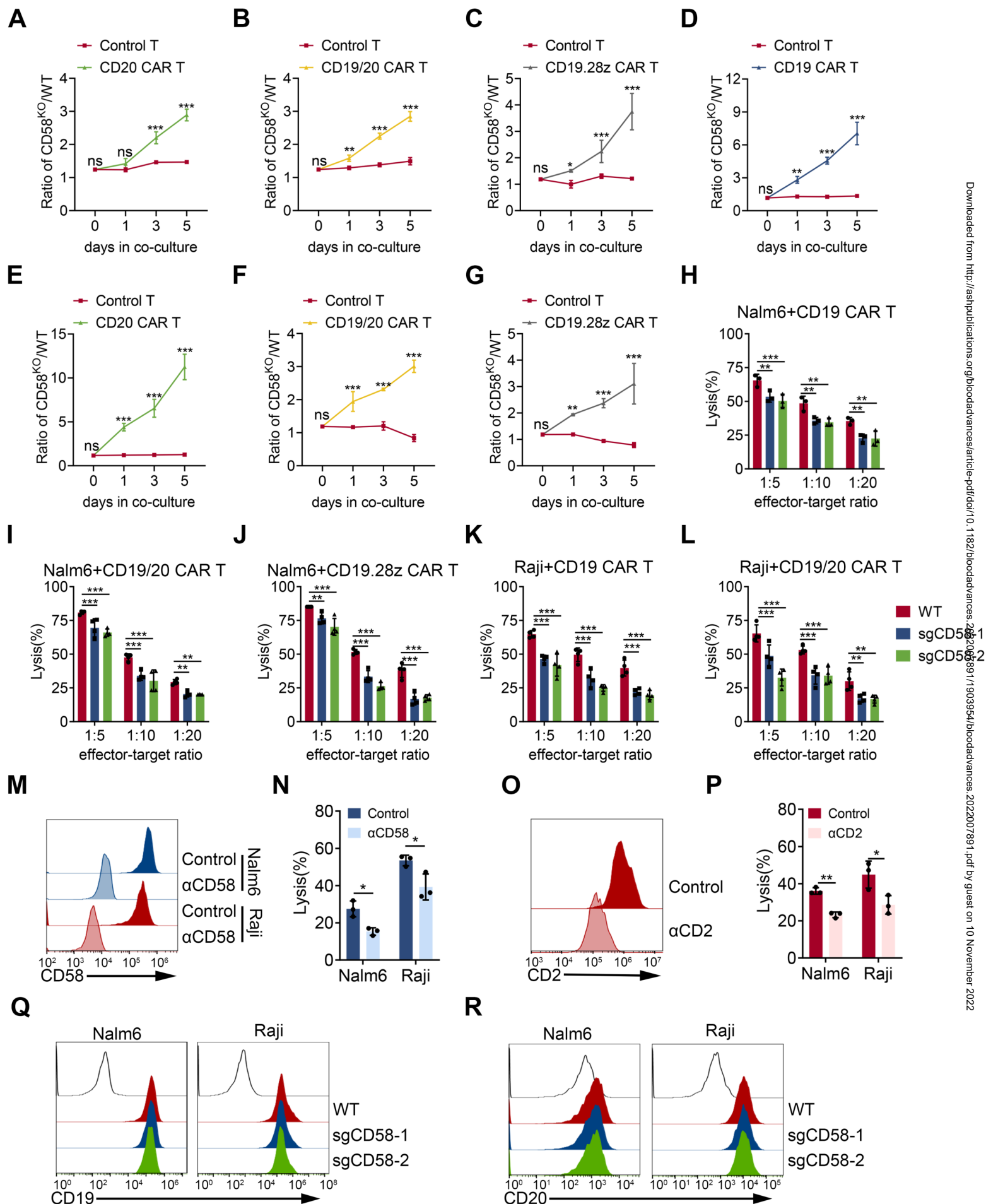
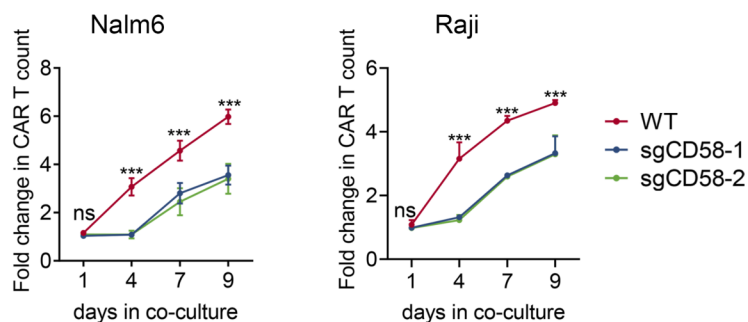
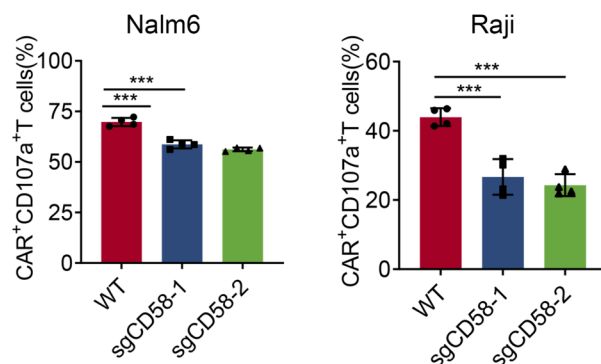


Figure 3

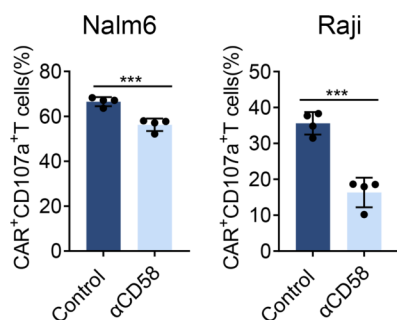
A



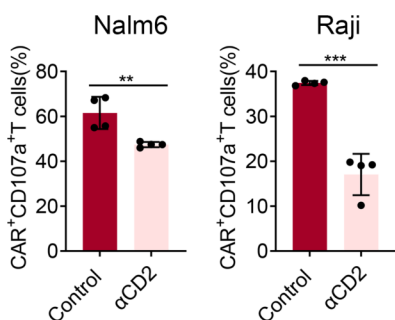
B



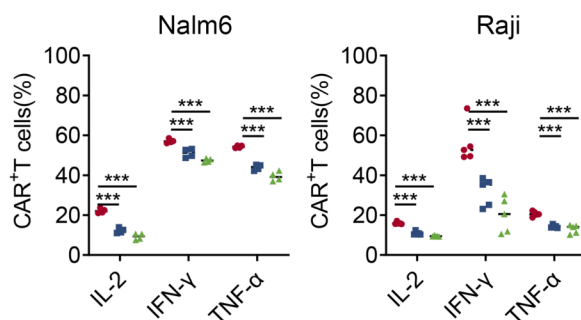
C



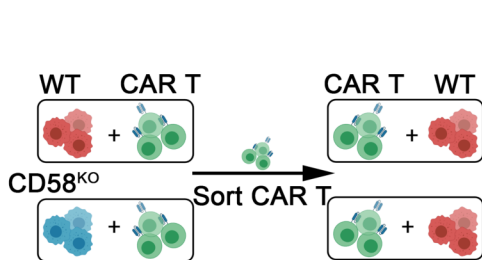
D



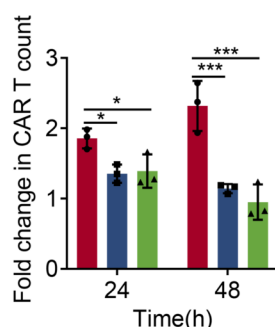
E



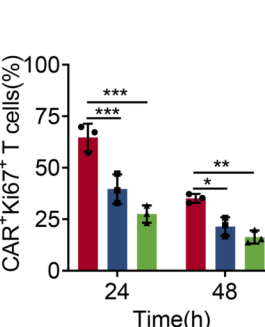
F



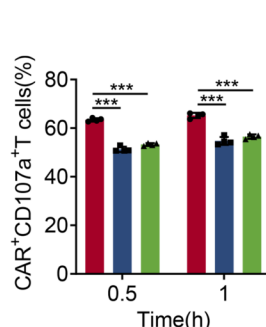
G



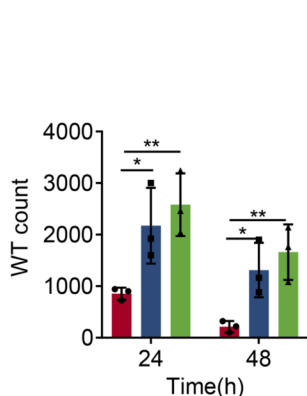
H



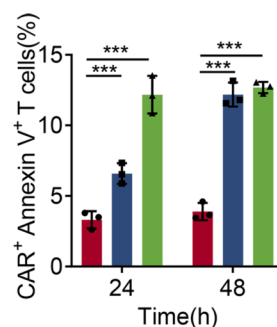
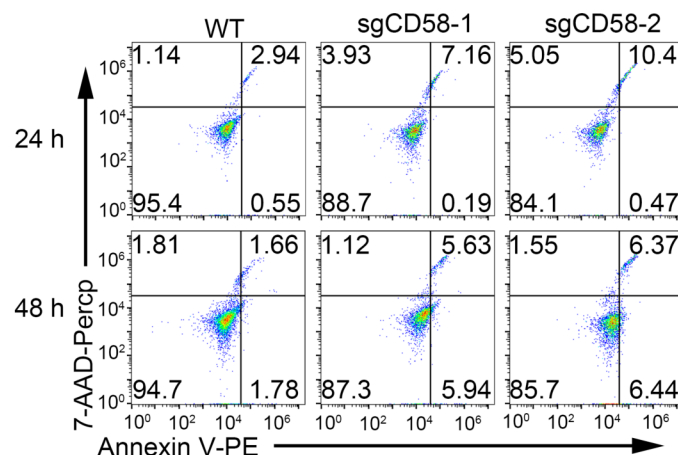
I



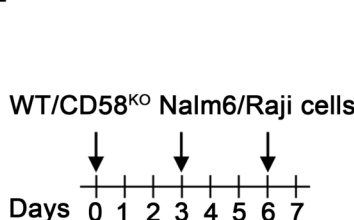
J



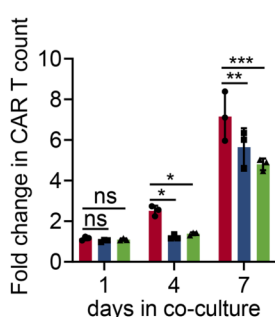
K



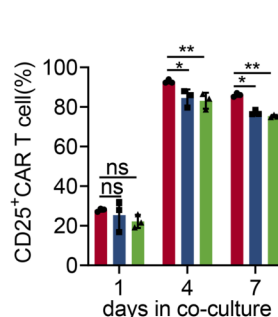
L



M



N



O

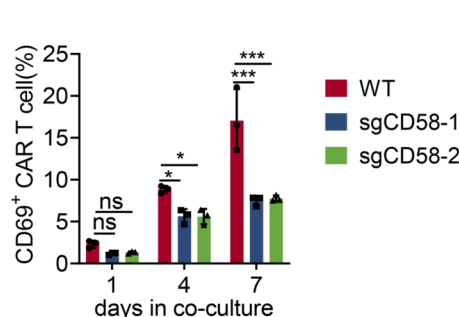
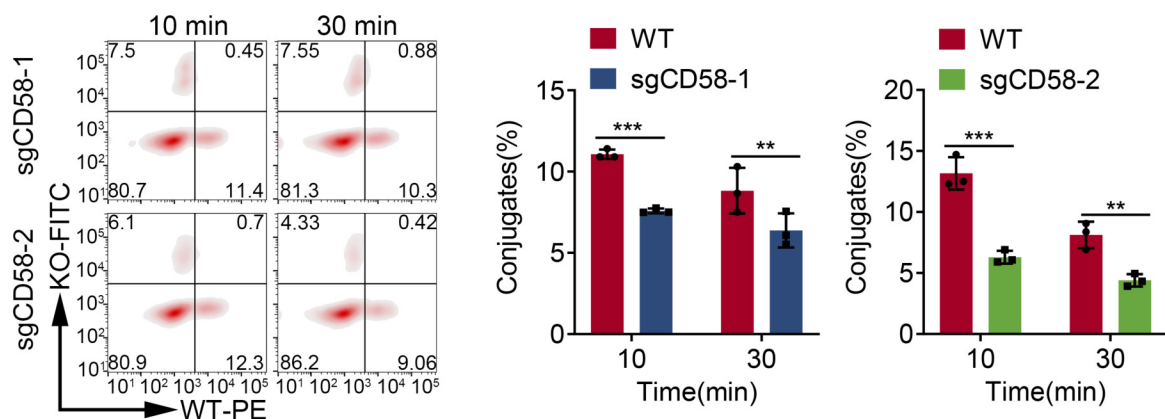
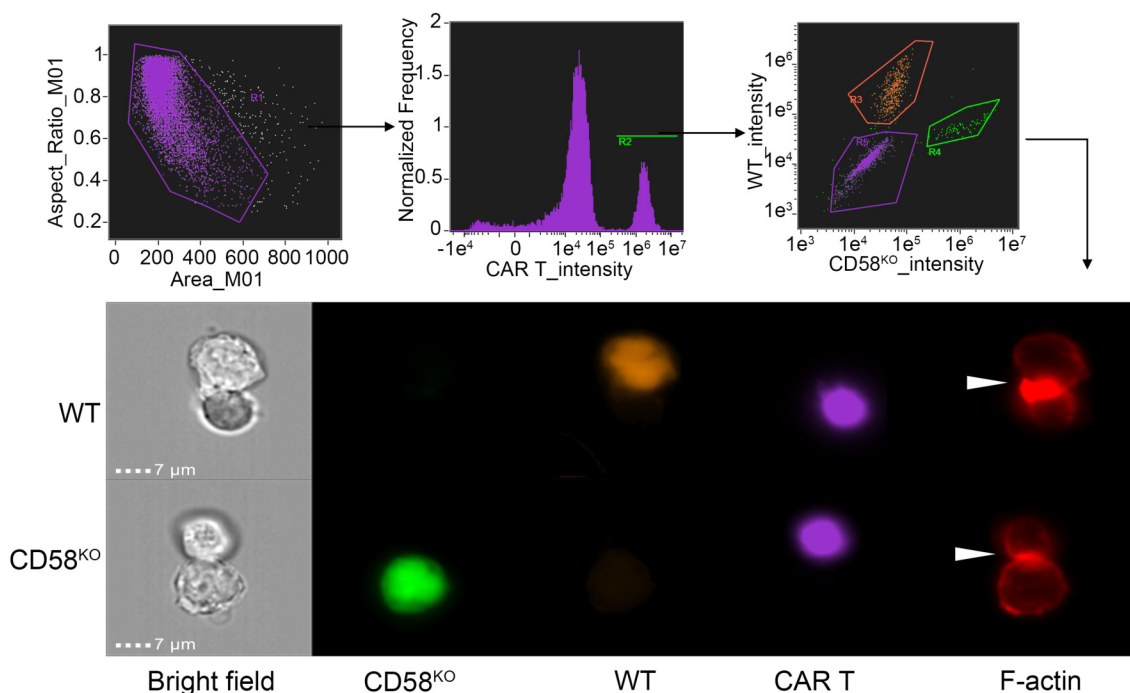


Figure 4
Figure 4

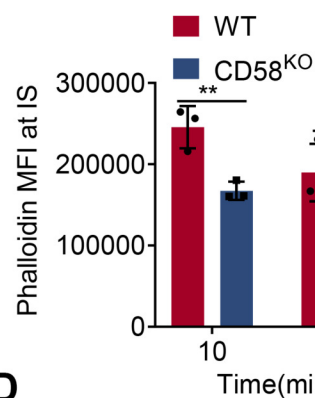
A



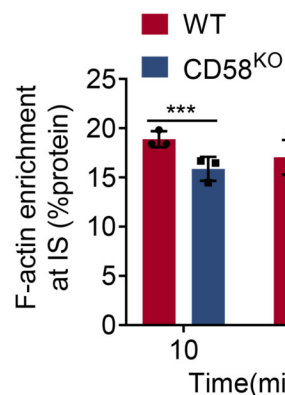
B



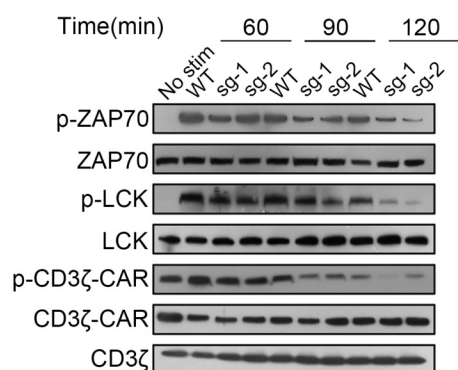
C



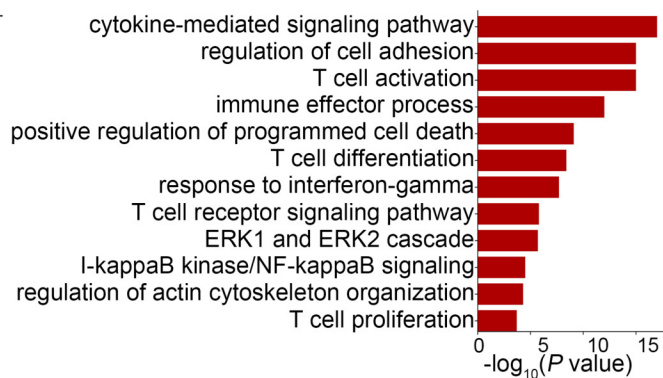
D



E



F



G

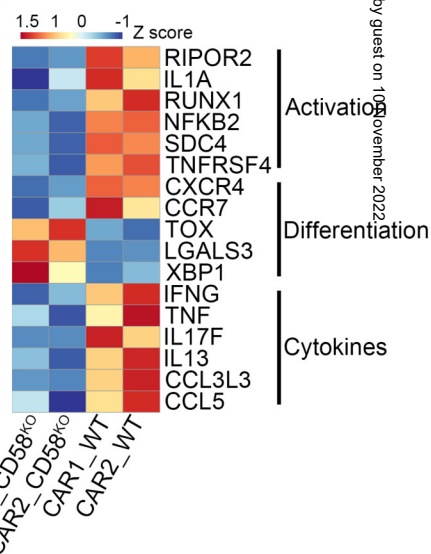
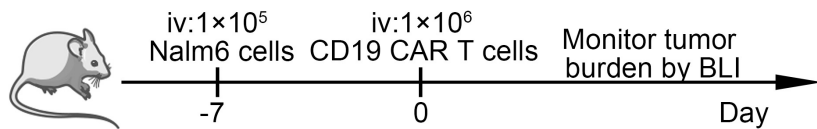


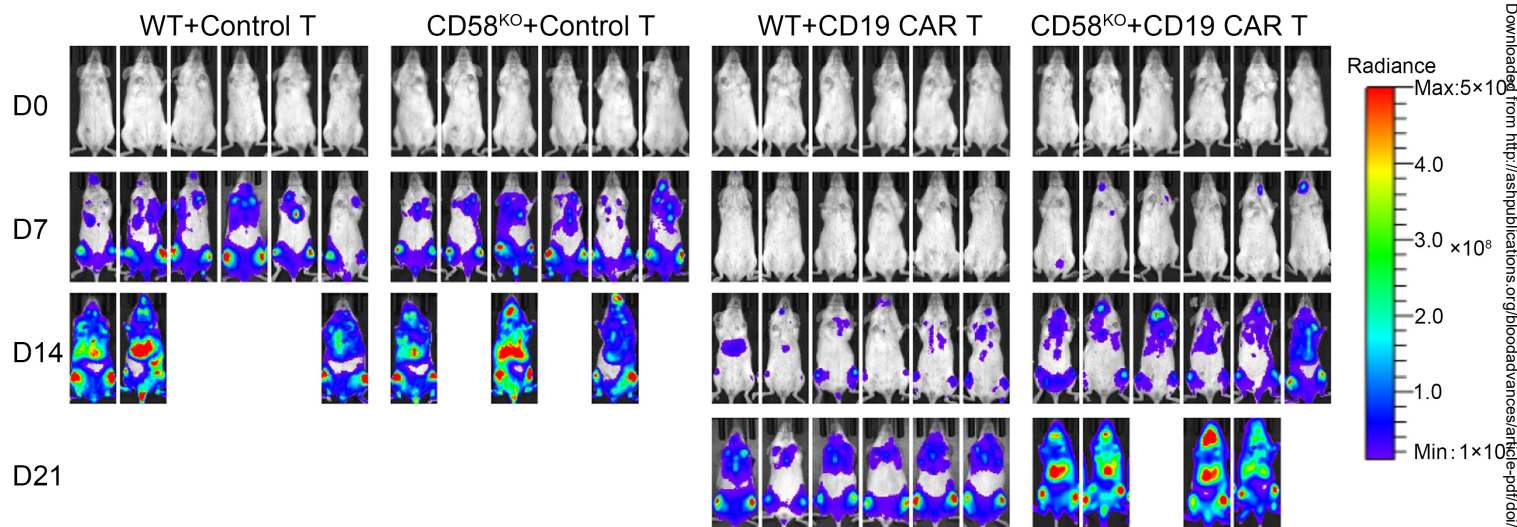
Figure 5

Figure 5

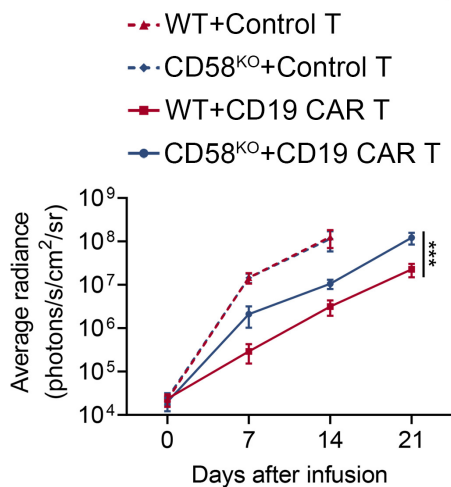
A



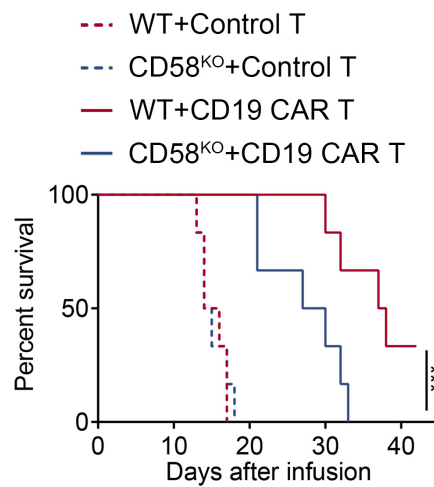
B



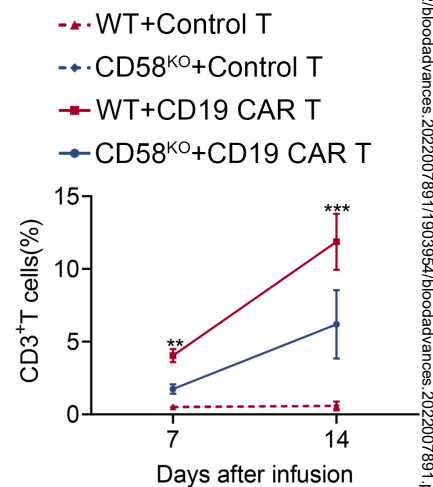
C



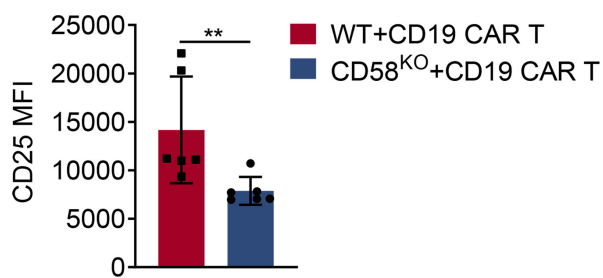
D



E



F



G

